ADVANCES IN NUCLEAR SCIENCE AND APPLICATIONS

Volume 1, No. 4 (2025), P. 250-268

Quarks in Hadrons and Nuclei Part II: Quark Structure of Nucleus

G. Musulmanbekov

Joint Institute for Nuclear Research, Dubna, Russia

Institute of Nuclear Physics, Almaty, Kazakhstan

e-mail: genis@jinr.ru

DOI: 10.63907/ansa.v1i4.53
Received: 25 August 2025

Abstract

In the framework of the semi-empirical quark model, SCQM, we construct nuclei from light to heavy ones. Nucleons inside nuclei are bound due to linkages of SU(3) color fields of quarks. According to SCQM, the arrangement of nucleons within nuclei reveals the emergence of the face-centered cubic (FCC) symmetry. Binding of nucleons are provided by quark loops which form three and four nucleon virtual clusters. Virtual alpha-clusters are responsible for binding energy enhancement in even-even nuclei. The model describes well most features of nuclei including their shapes, size and deformation.

1 Introduction

This Part II of the paper is aimed to give an answer to the question posed in Part I "Do quarks play the explicit role of arranging nucleons in the nuclear structure?". As mentioned in Part I [1], the theory of strong interactions, QCD, which ingredients are quarks and gluons, works well at small distances and high momentum transfers, that is typical in high energy processes. At the same time, it has many unsolved problems at large distances typical for the nuclear structure. Effective Field Theories, EFT, based on QCD, reduce the quark and gluon fields to a set of meson fields, so EFT approach does not touch the quark degrees of freedom of nucleons. Traditional models of nuclear physics, based on the nucleon-nucleon potential, face difficulties in attempts to describe the nucleon-nucleon interaction at short distances where they

are forced to include some undiscovered heavy mesons. Including three-body forces does not improve this approach even for light nuclei.

Historically there are three well known conventional phenomenological nuclear models based on different assumption about the phase state of the nucleus: the liquid-drop, shell (independent particle), and cluster models. The liquid-drop model requiring a dense liquid nuclear interior made up of protons and neutrons and aimed to predict nuclear radii, collective oscillations, etc., was effective to calculate nuclear binding energies [2, 3]. In contrast, in the shell model each point nucleon orbits in mean-field potential created by other nucleons; the model predicts nuclear spin and parity and shell-like orbital-filling [4]. The cluster models, describing the nucleus as a molecule-like collection of proton and neutron groups, require the assumption of strong local-clustering of particularly the 4-nucleon alpha-particle in order to make predictions about the ground and excited states of cluster configurations [5, 6, 7]. The dilemma of nuclear structure theory is that these mutually exclusive models work surprisingly well for qualitative and quantitative explanation of certain limited data sets, but each model is utterly inappropriate for application to other data sets.

A brief content of the paper is the following. We argue that nucleons within nuclei are bound to each other via SU(3) color quark–quark interactions which lead to strong nucleon–nucleon correlations. This is realized in the framework of the so-called Strongly Correlated Quark Model of the nucleon structure (SCQM) that was described in details in Part I [1]. The model, applied to build the nuclear structure, reveals the emergence of the face-centered cubic (FCC) symmetry. According to the model the binding of nucleons in nuclei are provided by quark loops which form three and four nucleon correlations. In difference with cluster models these correlations result in emergence of *virtual* (3- and 4-)nucleon clusters. We start building the nuclear structure from light to medium nuclei by constructing the nuclear shells in Section 2. Section 3 describes the details of the FCC lattice model and its relation to Independent Particle Model (IPM). In Section 4 we unite SCQM with FCC lattice model. Then we reformulate the model in terms of *virtual clusters* (Section 5).

2 Building the nuclear shells

As shown in Part I the nucleon represents a non-spherical triangular shaped object with three color quarks, and interactions between quarks within the nucleon arise due to destructive interference of their overlapped colour fields [1]. The same mechanism of quark–quark interactions is responsible for the nucleon–nucleon binding in nuclei. As shown in Part I, the interaction of quarks in a nucleon via overlap of their color fields can be considered as the action of the potential

$$U(x) = 0.36 \tanh^2(\alpha x) \tag{1}$$

on each quark. Different color fields of quarks belonging to the neighbour nucleons being overlapped create additional minima of the potentials in each nucleon with a small ($\sim 2\ MeV$) well depth, as we know from the binding energy of a deuteron (Fig. 1). As emphasized in Part I, the nucleon is a non-spherical, triangular shaped color object. Although, it is white, i.e. it's total color charge is zero, it possesses tricolor (Red, Green, Blue) quark ends on the periphery. It is *the color quark ends that bind nucleons together in nuclei.*

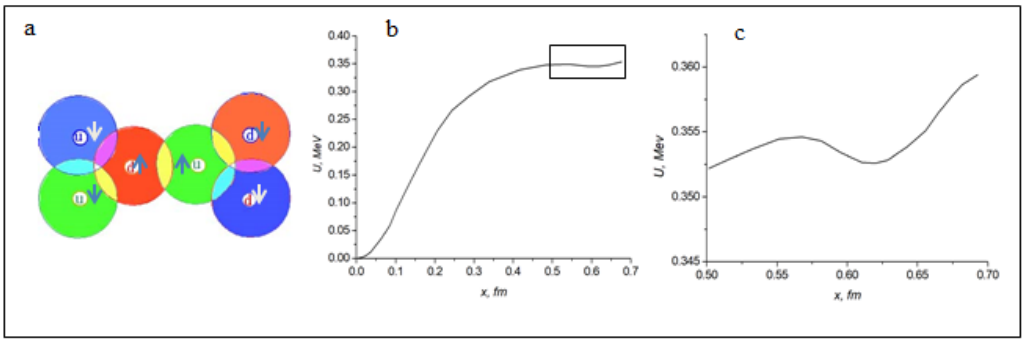

Figure 1: Overlap of quark color fields between proton and neutron in a deuteron (on the left) leads to emergence of an additional minimum in the quark potential for both interacting quarks (on the middle); the selected part of the potential is shown at a larger scale on the right.

With regards to the spin and flavor alignment of adjacent quarks, we should take into account the fact that the multiquark states of 6, 9, 9, and 12 quarks in ^2H, ^3H, ^3He and ^4He belong to the completely antisymmetric representation of the $SU(12)$ group which contains the direct product

$$SU(2)_{flavor} \otimes SU(2)_{spin} \otimes SU(3)_{color}. \tag{2}$$

That is, up to 12 quarks (in the case of ^4He) can occupy the s-state. Most quark configurations in the above multiquark systems built according to group representations correspond to, so-called, "hidden color" states as these can not be represented in term of the free (color-singlet) nucleons [8]. We restrict the multiquark configurations by only the color-singlet clusters–nucleons. In that way, two nucleons will be bound by overlapping quark color fields if the following **selection rules** are satisfied on these interacting quarks:

1) $SU(3)_{color}$ – antisymmetric,
2) $SU(2)_{isospin}$ – antisymmetric,
3) $SU(2)_{spin}$ – symmetric.

The first two rules are specified by assumption that colors and flavors of quarks at a linkage must be antisymmetric. The third rule implying parallel spins of the quarks at a linkage is defined by combinatorics for 12 quarks in ^4He. Applying these rules one can start to construct nuclei. The three-nucleon system is formed by the linkage of two quarks ends of each nucleon with quark ends of two other nucleons according to the above rules. Three-nucleon nuclei, namely ^3H and ^3He, represent triangular configurations with one quark loop and three quarks free ends (Fig. 2). One may notice that interaction of two color quark ends produces in the overlap region (linkage) corresponding anticolor. It follows from $SU(3)_{color}$ symmetry where a pair of quarks has coupled representations $3 \otimes 3 = 6 \oplus \overline{3}$. The total color charge of anticolors in the loop is zero. Completion to a four-nucleon system, ^4He, from three-nucleon one is realized by binding the free quark ends in ^3H (^3He) with the three quarks of an additional proton (neutron) again in accordance with the above rules (Fig. 3). As a result, oblate, triangular–shaped nucleons in ^4He settle on the faces of octahedron (Fig. 3 a) and linkages of quarks of neighbour nucleons create

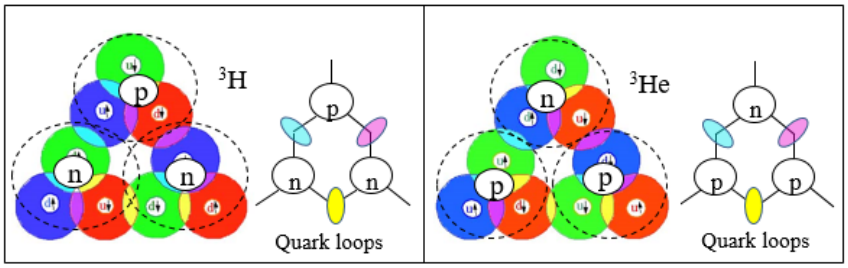

Figure 2: Quark representation of three–nucleon systems, ^3H and ^3He. Quark loops emerging due to overlap of quark color fields are shown on right sides of each nucleus.

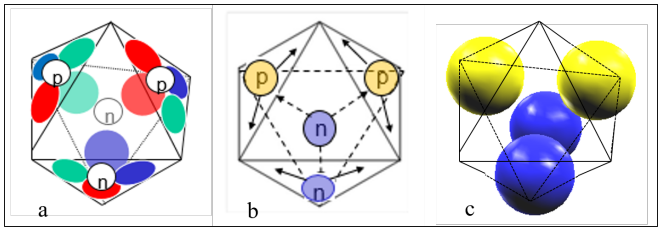

Figure 3: Three octahedron-shaped representations of ^4He: a) color quark representation, b) nucleons with quark ends forming 4 quark loops and c) nucleons as spheres.

four loops (Fig. 3 b). For further convenience nucleons are depicted as spheres (Fig. 3 c). This representation, as we will see below, is justified not only by the convenience of presentation but formation in the nuclear structure of so-called "virtual clusters". It must be noticed that starting from three nucleon system the amplitude of quark oscillation inside nucleons is restricted within the small potential well (Fig. 1) created by overlapping quark color fields of neighbour nucleons, and the quarks become constituent with a mass $\sim 1/3$ of the nucleon mass. From experiment we know that ^4He is not only a compact nucleus but it possesses much more binding energy in comparison with nearby nuclei. As it is known from the experiments (Table 1), the

Table 1: Relation of binding energy to quark loops and unbound quark ends

Nucleus	E^{exp}_{bind}/bond, MeV	Quark loops	Unbound quark ends
^2H	2.2	0	4
^3H	2.83	1	3
^3He	2.57	1	3
^4He	7.07	4	0

binding energy per nucleon is minimal for the deuteron and maximal for the ^{4}He nucleus. This variability is caused by the number quark loops and/or the number of

unbound or free quarks ends. The quark or color loop is created by the linkage of the quark ends of three nucleons, as in ^{3}H and ^{3}He. The fewer unbound/free quark ends, the greater the binding energy between nucleons. Conversely, the more free quark ends, the lower the binding energy. The maximal binding energy of ^4He is due to the presence of four quark loops, binding all quark ends of the four nucleons. Therefore, reducing the number of free quark ends in multinucleon system *deepens*

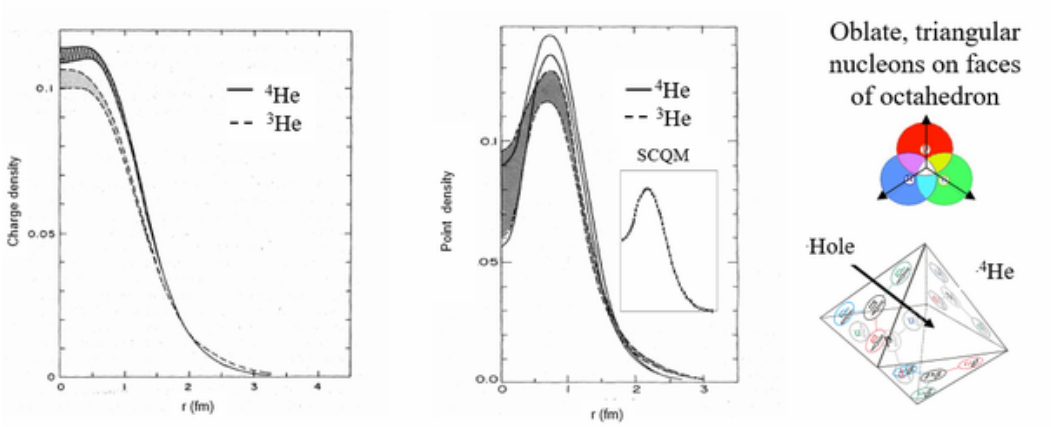

Figure 4: Electron scattering data on ^3H and ^4He charged density distributions (left plot) and corresponding point particle distributions [9] (right plot) with our SCQM calculation (embedded plot). On the right side: the geometrical shape of ^4He, octahedron, with the hole inside it.

the potential well and increases the binding energy between nucleons. Calculating the depth of the potential well for systems of two, three and four nucleons, taking into account the overlap of the color fields of quarks, is a separate task that needs to be solved in the future. This task is closely related to the problem of three- and four-particle forces, since the quark loop in ^3H and ^3He, and four loops in ^4He are explicit realization of these forces. Four quark loops in ^{4}He enclosing free color quark ends minimize colority of the nuclear system. In that sense two- and three-nucleon systems possessing 4 and 3 color quark ends are colored objects. Hence, in order **to construct stable nuclei it is necessary to bind all three quark ends of each nucleon**. The first nucleus where all three quark ends of each of the four nucleons are bound to the quarks of the other three nucleons is the ^4He nucleus. To separate one nucleon from ^4He, three bonds (quark ends) must be broken, each of which accounts for about 7 MeV (see Table 1). This agrees with the experimental value of $\sim$ 20 MeV.

Because of geometric shapes of ^3H, ^3He and ^4He there should be **depression** or a **hole** in the center of their nuclear matter distributions. This peculiarity of 3- and 4-nucleon systems shown on Figure 4 has been found out in a model independent analysis of electron scattering data performed by I. Sick and co-authors [9]. On the other hand ^4He is the most compact nucleus with the size which is less that sizes of ^3H and ^3He. These distinctive features of 3- and 4-nucleon systems together with the hole are a consequences of the non-spherical, oblate shape of the nucleon.

Starting from the structure of the ^4He all nuclei possess crystal-like structure. Indeed, in ^4He a pairs of (oblate) protons are located on the upper opposite faces of the octahedron and a pair of neutrons — on opposite faces of its lower half. In this geometrical configuration four nucleons are in s state that corresponds to the

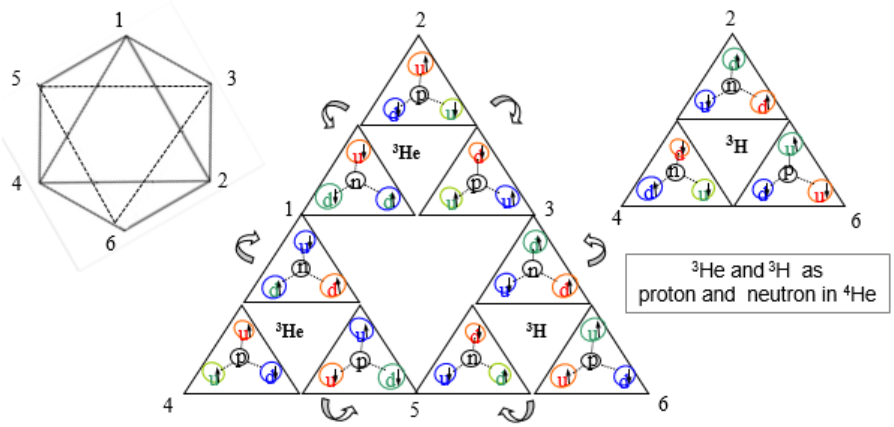

Figure 5: Quark configurations in unfolded faces of the p-shell. ^3H and two ^3He in the central figure correspond to three faces of p-shell octahedron (on the left). Turning these faces around the lines 1–3, 1–5, 3–5 and connecting vertices 2, 4, 6 with the same ones of ^3H (on the right), corresponding to the fourth face of octahedron, we get the p-shell.

first s shell of the shell model. Next, the p shell can be represented as a larger octahedron, nesting ^{4}He octahadron, with two ^3He triangles instead of protons and two ^3H triangles instead of neutrons. They are arranged in a way to form alternating neutron-proton or proton-neutron layers. The quark configurations of the $p-$shell satisfying above three selection rules are shown in unfolded faces of the $p-$octahedron on Figure 5. Quarks are depicted as red, blue and green ends of nucleons with corresponding spins. Two ^3He and two ^3H triangles are located

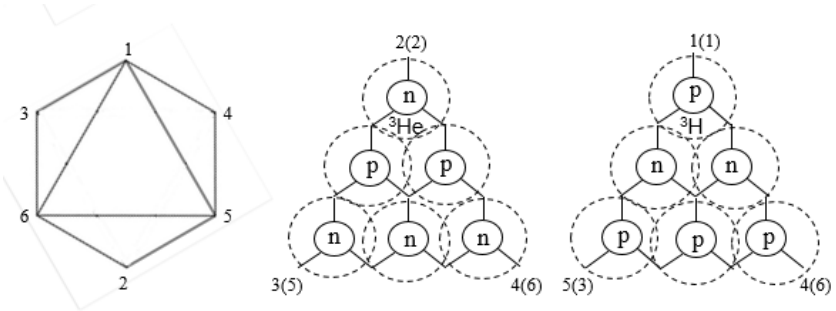

Figure 6: Building the $d-$shell: two upper faces of the octahedron (on the left), 1-4-5 and 1-3-6, are covered by the configuration of nucleons shown on the right; two lower faces, 2-3-4 and 2-5-6, – by the configuration in the middle.

parallel to empty faces of the ^4He octahedron, and the free quark ends of these triangles are coupled as in the ^4He octahedron. This octahedron with the nested ^4He octahedron represents the nucleus of ^{16}O. The next shell with principal number $n = 2$ is constructed in a similar way as the alternating proton-neutron (neutron-proton) layers by expanding the previous triangles adding a row of three protons to the row of two neutrons in ^{3}H and a row of three neutrons to the row of two protons in ^{3}He (Fig. 6). Here we dropped the quark content because of complexity of the representation. And again, these triangles are arranged in pairs on opposite faces of the octahedron which are parallel to the unoccupied faces of the nested $p-$octahedron. All three shells corresponding to ^{4}He, ^{16}O and ^{40}Ca nuclei are shown in Figure 7 where nucleons are represented by spheres. The centers of the

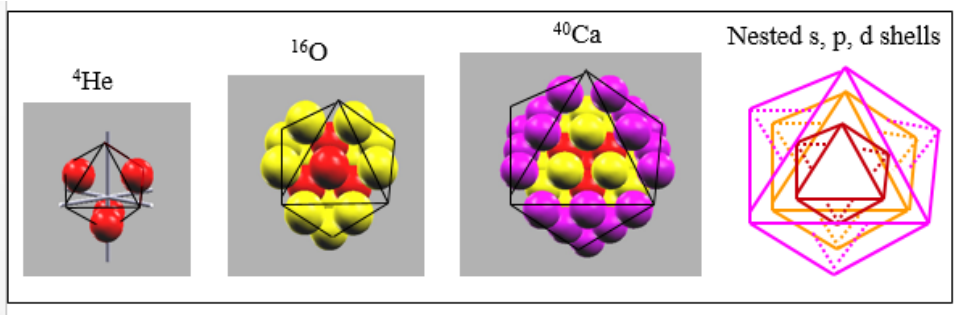

Figure 7: ^{4} He, ^{16} O and ^{40} Ca nuclei composed of nucleons colored by red ($s-$ shell), yellow ($p-$ shell) and magenta ($d-$ shell); on the right, $s-, p-, d-$ shells depicted as nested octahedrons.

spheres coincide with the centers of mass of the quarks in the nucleons. They are also shown in Figure 8 in isospin representation with proton and neutron alternating layers. Surprisingly, the arrangement of nucleons produced by quark-quark interactions

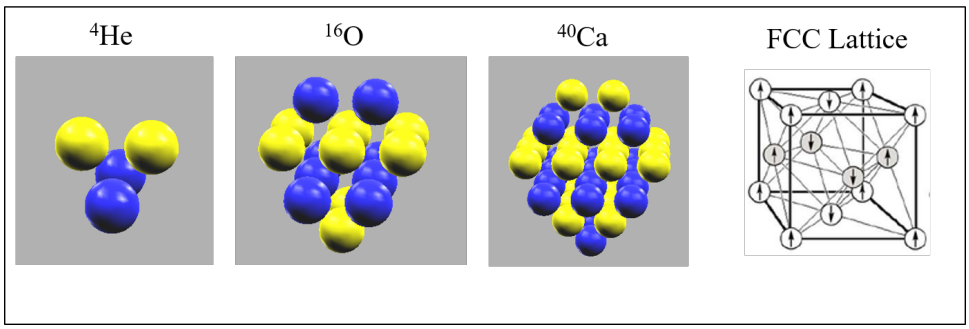

Figure 8: ^{4} He, ^{16} O and ^{40} Ca nuclei as alternating proton (yellow) and neutron (blue) layers. The FCC lattice unit with alternating spin and isospin layers (on the right); protons are gray, neutrons are white (or vice versa).

corresponds to a regular lattice, namely, Face Centered Cubic lattice (FCC) which is one of two close-packing lattices (on the right in Figure 8). Moreover, besides the alternating isospin layers nucleons are arranged in the alternating spin layers. Spins are indicated by the arrows on the nucleons.

3 FCC Lattice model of the nuclear structure

Thus, our model, being applied to the nucleus leads to the arrangements of nucleons corresponding to the symmetry of the FCC Lattice. The idea to represent the atomic nucleus as a lattice with nodes occupied by nucleons has a long history. In 1937, long before the advent of the Independent Particle Model (IPM) or/and shell model, the nobel laureate E. Wigner [10], studying the symmetry of the nuclear Hamiltonian in Cartesian coordinates, obtained a discrete symmetry of nuclear multiplets, which subsequently coincided with the symmetry of the FCC Lattice. More than a decade after Wigner's paper the idea of nucleons orbiting under a central potential was formulated by Mayer and Jensen in their Independent Particle (IPM) or Shell model [4]. Later on several authors continued to develop the FCC lattice representation of nuclear structure [12, 13, 11, 14, 15]. They demonstrated that this representation is

identical (with some differences) to IPM. M. Gillard with coauthors modified the skyrmion model of the nuclear structure where skyrmions as particles are located on the FCC vertices [16, 17].

In order to connect our model with the quantum numbers of the shell model, we follow the nuclear FCC Lattice model formulated by N. Cook and V. Dallacasa [15]. The time-independent Schrödinger wave-equation for describing a particle reads

$$-(\frac{\hbar^2}{2m})(d^2\Psi/dr^2) + V(r)\Psi(r) = E\Psi(r). \tag{3}$$

The solutions that satisfy this equation in the one-dimensional case have a quantum number, n, that specifies the number of sine-waves. Using the idea of a harmonic oscillator, the energy of each state can then be defined as:

$$E_n = \hbar w_0(n + 1/2) \qquad n = 0, 1, 2, 3, ... \tag{4}$$

Assuming the particle is confined to a 3D box, (3) can be rewritten to define the particle's position in Cartesian coordinates:

$$-(\frac{\hbar^2}{2m})(d^2\Psi/dx^2 + d^2\Psi/dy^2 + d^2\Psi/dz^2) + V(r)\Psi(r) = E\Psi(r). \tag{5}$$

The solutions of (5) for the three-dimensional harmonic oscillator can be described in terms of three numbers, n_x, n_y, n_z. The total energy is then 3-fold the one-dimensional case:

$$E_n = \hbar w_0(n_x + n_y + n_z + 3/2) = \hbar w_0(n + 3/2) \qquad n = 0, 1, 2, 3, ... \tag{6}$$

In other words, the energy states in three dimensions depend only on the sum n, which is called the principal quantum number. Different combinations of n_x, n_y, n_z that give the same total $n-$ value denote spatially distinct "degenerate" states, with the same energy. By defining the allowed states as all *odd-multiples* of sine waves, a set of oscillatory states within the box are found to have occupancies related to the known energy levels of the nucleus. The first three shells ($n = 0, 1, 2$) are listed in Table 2, together with the occupancies produced by the so-called degeneracy of spin and isospin. As the nucleon moves to higher shells, its energy level increases in

Table 2: Energy levels of a particle confined in a 3D box ([11], p. 179)

Energy $E/\hbar w_0$	$n-$shell $(n_x + n_y + n_z$ - 3)/2	Wave functions (n_x, n_y, n_z)	No. of Distinct Wave functions	Spin Degeneracy	Isospin Degeneracy	Total Occupancy
7/2	2	(511)(151)(115) (331)(133)(313)	6	12	12	40
5/2	1	(311)(131)(113)	3	6	6	16
3/2	0	(111)	1	2	2	4

discrete jumps (3/2, 5/2, 7/2, . . .). At the same time, the number of nucleons that can reside at each level increases due to the fact that the number of permutations of the coordinate indices increases (third column in Table). Prior to consideration of the

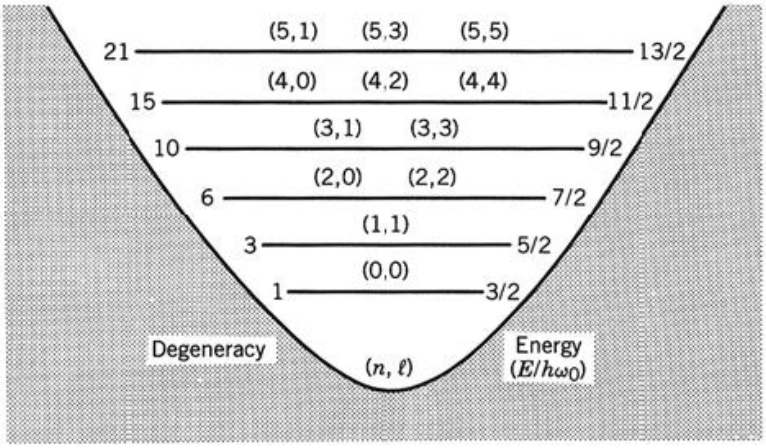

Figure 9: The energy levels and degeneracy of the harmonic oscillator potential that is the basis of the shell model ([18], p. 33); n and l are the principal and orbital quantum numbers.

degeneracies brought by spin and isospin, there are 1, 3, 6, etc. states for higher levels (fourth column in Table). In the framework of the shell model, energy states generated using the harmonic oscillator potential are shown in Fig. 9. The occupancies of the various energy levels obtained through combinations of the principal, n, and orbital, l, quantum numbers are identical to those obtained with n_x, n_y, n_z using Cartesian space. But, as seen in Table there is further degeneracy caused by spin and isospin. For every distinct state, each nucleon can exist in either a spin-up or spin-down state and there are two types of nucleon – protons and neutrons (isospin-up or isospin-down) – that can co-exist in each state. The wave-function subscripts in Table, (n_x, n_y, n_z), are the absolute values of the integers corresponding to one octant of Cartesian space, but can be generalized to all nucleon coordinates, using permutations of positive and negative coordinates depending on the shell number. It means four times the number of states are allowed in each n-shell of the Schrödinger equation (fifth and sixth columns).

Although the IPM reproduces a table similar to Table 2, it usually accounts the spin (fifth column), and not the isospin degeneracy. The IPM requires one further assumption, spin-orbit coupling, in order to explain the empirical shell structure of the nucleus. That is, the total angular momentum of each nucleon is assumed to be the sum of the nucleon's intrinsic spin and its orbital angular momentum, $j = l \pm s$, that is experimentally observable. The known sequence of $j-$ levels then matches well with the shell model sequence.

Let us now look at how that nucleon build-up sequence might be represented in a lattice of nucleons. The first shell represented by four spherical nucleons possesses the tetrahedral symmetry. If the origin of the coordinate system is taken as the center of a tetrahedron and all additions of nucleons to the central tetrahedron are in accordance with a face-centered-cubic close-packed lattice, then it is found that the closure of each consecutive, symmetrical $(x = y = z)$ geometrical shell in the lattice corresponds precisely to the numbers of nucleons in the shells derived from the three-dimensional Schrodinger equation, as listed above. According to the FCC Lattice Model a nucleon's principal number, n, is a function of the nucleon's distance

from the center of the lattice – leading to the shells for each consecutive n eigenvalue:

$$n = (|x| + |y| + |z| - 3)/2, \tag{7}$$

where x, y, z are odd integers. The first shell (s shell) contains four nucleons with coordinates 111, -1-11, 1-1-1, -11-1. The second shell (p shell): 12 nucleons 31-1, 3-11, -311, -3-1-1, 1-31, -131, 13-1, -1-3-1, -113, 11-3, 1-13, -1-1-3. The third shell (d shell) contains 24 sites that are permutations of ± 1, ± 3 and ± 5. The total angular momentum value of a nucleon in the lattice

$$j = (|x| + |y| - 1)/2 \tag{8}$$

is defined in terms of the distance of the nucleon from the spin axis of the system – leading to roughly cylindrical j subshels within each n shell. The azimuthal quantum number is a function of the nucleon's distance from a central plane through the lattice

$$m = (|x|/2)(-1)^{x-1}. \tag{9}$$

The sign of m is determined by the nucleon spin defined relative to the x-axis

$$s = (-1)^{x-1}/2. \tag{10}$$

The isospin of nucleons is defined relative to the z-axis

$$i = (-1)^{z-1}/2. \tag{11}$$

Parity can be defined in the lattice as the product of the signs of nucleon coordinate values:

$$p = sign(x)sign(y)sign(z), \tag{12}$$

and the parity of the entire system is simply the product of all $i-$ th nucleon parities:

$$p_A = \prod(sign(x_i)sign(y_i)sign(z_i)) \tag{13}$$

Parity in the lattice therefore alternates between positive and negative in successive $n-$ shells. Thus, all shells and subshells of the well established IPM have geometrical interpretations. Correspondence of the shells and subshells between the IPM and the FCC Lattice model is shown in Figure 10.

	n-shells $n = (\|x\| + \|y\| + \|z\| - 3)/2$						j-subshells $j = (\|x\| + \|y\| - 1)/2$							m-subshells $m = \|x\|/2$							
	0	1	2	3	4	5	$\frac{1}{2}$	$\frac{3}{2}$	$\frac{5}{2}$	$\frac{7}{2}$	$\frac{9}{2}$	$\frac{11}{2}$	$\frac{13}{2}$	$\frac{1}{2}$	$\frac{3}{2}$	$\frac{5}{2}$	$\frac{7}{2}$	$\frac{9}{2}$	$\frac{11}{2}$	$\frac{13}{2}$	Total
	2						2							2							2
								4						2	2						6
		6					2							2							8
No. occupancies									6					2	2	2					14
								4						2	2						18
			12				2							2							20

Figure 10: The shells and subshells and their occupancies in the IPM and in the FCC Lattice model ([11], p. 188).

However, in the IPM a build up procedure applies separately to protons and neutrons, and as a result the isospin degeneracy (6-th column in Table 2) is absent. This suggests that protons and neutrons are not correlated in any way, which is one of the foundations of the model. This is one of the main drawbacks of the model and many efforts are made to take into account nucleon-nucleon correlation as residual interactions.

4 SCQM on FCC lattice

Now we can assign FCC coordinates to the nucleons of the $s-$, $p-$, $d-$ shells (Fig. 7) constructed using quark-quark interactions. As seen in Figure 11 the nuclei with these closure shells can be built in the FCC coordinate system with the origin taken as the center of the $s-$ tetrahedron/octahedron. Now any nucleon has a unique position in three-dimensional space. Moreover, the nucleon's lattice position defines a unique set of quantum values n, j, m, s, i, p (Eqs. (7) - (12) and Fig. 10)). To generate the coordinates of nucleons and their quantum numbers, we used the computer program, so-called Nuclear Visualization Software which we substantially revised [15].

We obtained a remarkable result: constructing the nuclear shells by overlapping of SU(3)-colored quark fields led to the nuclear structure emerging from the solution of the Schrodinger equation for harmonic oscillator in three-dimensional Cartesian coordinates. Moreover, it gives the total occupation numbers with all degeneracies, including isospin states. Thus, our model of strongly correlated quarks applied to

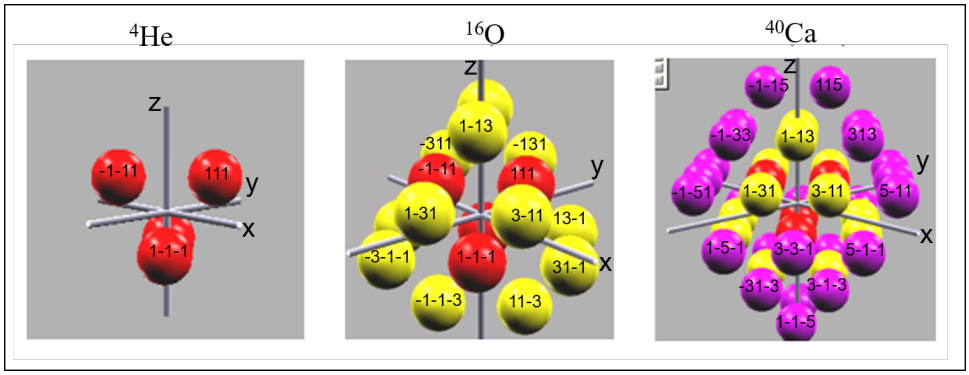

Figure 11: ^{4}He, ^{16}O and ^{40}Ca nuclei in the FCC lattice. Nucleon's colors denote different $n-$shells: red ($n = 0$), yellow ($n = 1$) and magenta ($n = 2$). Each nucleon's $n-$value is a function (7) of its $x-$, $y-$ and $z-$coordinate values.

the description of the nuclear structure reveals several important points:

1) The model justifies the FCC lattice model, which suffers from the lack of grounds for the bonds between nucleons in the lattice.
2) All nucleons in a nucleus are strongly correlated with each other. Correlations occur not only between nucleons of the same type (proton-proton, neutron-neutron), but also between protons and neutrons.
3) The model leads to a dense packing of nucleons in the central region, which corresponds to the experimental fact that the size of the nucleus is determined by the number of nucleons in it.
4) Since the nucleons occupy fixed lattice sites, at first glance, they seem to violate the quantum-mechanical uncertainty principle. This argument against the lattice arrangement of nucleons is reduced by the fact that, in accordance with the SCQM, nucleons are nonlinear standing waves of quark fields, the amplitude of which is limited by a potential well formed by the overlap of the quark color fields of neighboring nucleons (Fig. 1).

While constructing the nuclear structure we dealt only with the closure-shell nuclei up to ^{40}Ca. But what about nuclei with unfilled shells, and what about heavier

nuclei whose shells begin to differ from those that given by the harmonic oscillator potential due to the excess of neutrons over protons, caused in turn by Coulomb interactions? To answer these questions we reformulate our model in term of *virtual* three- and four-nucleon clusters.

5 Nucleus as an aggregation of virtual clusters

Since nuclei immediately following ^{4}He have lower binding energies, we start with the ^{12}C nucleus which binding energy per nucleon (7.68 MeV) is significantly higher than for the ^{4}He nucleus (7.07 MeV). Such a large binding energy is a problem for explanation within the shell model. In the FCC lattice the ^{12}C nucleus can be built by removing two protons from the bottom and two neutrons from the top of $p-$ shell of the ^{16}O (Fig. 12). Here we put forward the main hypothesis about the

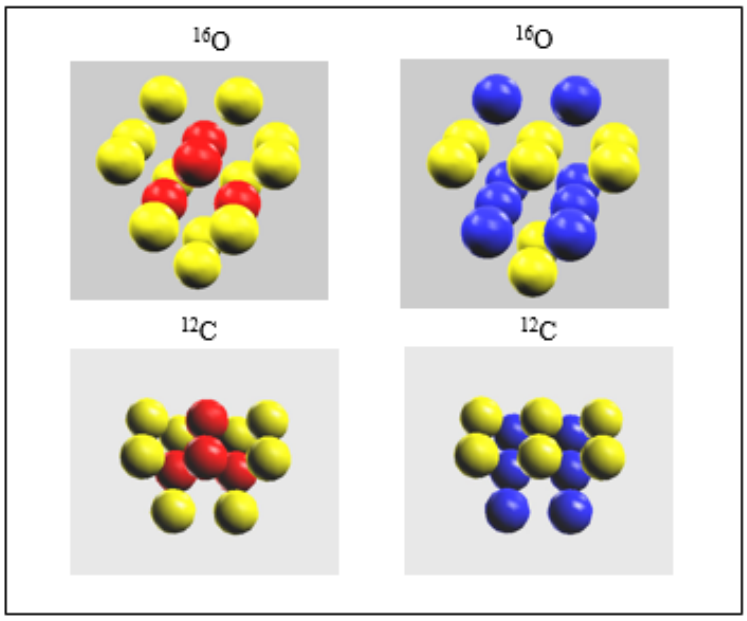

Figure 12: The ^{12}C nucleus built by removing two protons from the bottom and two neutrons from the top of $p-$ shell of ^{16}O. Left column: the shell/subshell representation; right column: the isospin representation; protons are yellow, neutrons are blue.

structure of the atomic nucleus: the bonding of nucleons in the atomic nucleus is a consequence of the *formation of virtual three- and four-nucleon clusters due to quark loops*. Let's look at the configuration of nucleons in the carbon nucleus from the point of view of the formation of alpha cluster aggregations. A close look at the ^{12}C nucleus in Figure 13 shows that the closest three protons, two of which are in the $p-$ shell and one in the $s-$ shell, together with four neutrons, two of which are in the $p-$ shell and the other two in the $s-$ shell, form two alpha clusters. Here the proton of the $s-$ shell becomes common or exchangeable to both alpha clusters. We call these alpha clusters virtual, since two adjacent alphas exchange a common nucleon, which in the process of exchange becomes a constituent of first one, then the other alpha cluster (Fig. 14). In the ^{12}C nucleus consisting of 12 nucleons, 4 virtual alpha clusters are formed, where four nucleons of the $s-$ shell

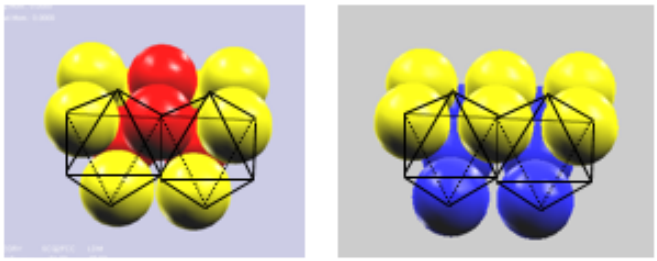

Figure 13: Formation two adjacent virtual $\alpha-$ clusters in the ^{12}C nucleus. Left column: nucleons in the shell/subshell representation (red – s-shell, yellow – p-shell); right column: the isospin representation (yellow – protons, blue – neutrons).

are exchangeable for each virtual alpha pair (on the right in Figure). Four blue transparent spheres depict the virtual alphas. From the quark-quark interaction point of view, a non-spherical triangular shaped nucleon, precessing due to its spin in the magnetic field of neighboring nucleons, ends up alternately on the faces of adjacent alpha octahedra, which leads to strengthening of internucleon bonds. During the spin precession, a non-spherical nucleon sweeps out most of the surface of a sphere. Therefore, in the region of nuclear density saturation, where almost all nucleons become exchangeable, they can be seen as **spherical** objects with a radius corresponding to the average size of a nucleon. The non-spherical, triangular shape of a nucleon manifests itself on the surface of a nucleus. It is this shape of a nucleon that leads to a comparatively small size of the alpha particle and an anomalously large size of a nuclear halo.

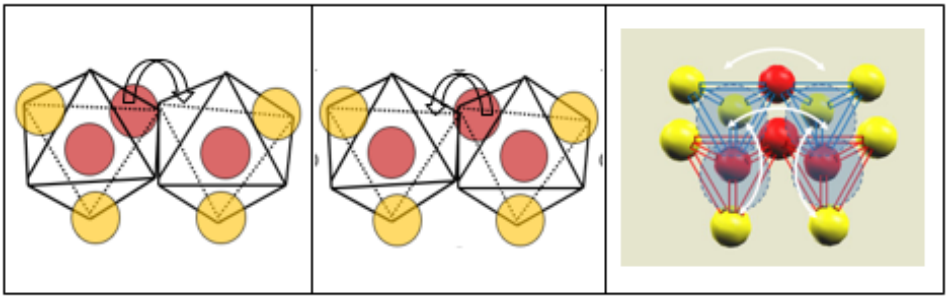

Figure 14: The exchange of a nucleon between two adjacent virtual $\alpha-$ clusters (left and middle). Right: the formation four virtual $\alpha-$ clusters in the ^{12}C nucleus.

If in a real alpha particle (Fig. 3) there are three bonds for each triangular nucleon, then in a nucleus like carbon, the effective number of bonds of the exchange nucleon increases because of the increasing number of virtual alphas, and this leads to an increase in the binding energy on average per nucleon. The higher the atomic number of a nucleus, the more virtual alpha clusters are formed in it, the more nucleons become exchangeable and the more (effective) bonds they acquire. For example, two protons in the bottom and two neutrons in the top of p-shell of ^{16}O (Fig. 11) form additional two virtual alpha clusters with two neutrons and two protons correspondingly of s-shell resulting in 6 virtual alphas. Further, nucleons of d-shell in ^{40}Ca (Fig. 11) form with nucleons of p-shell 22 additional virtual alphas which gives a total of 28 virtual alpha clusters. The formation of virtual alpha-clusters causes the inner shells making up the core of a nucleus to blur and

even disappear.

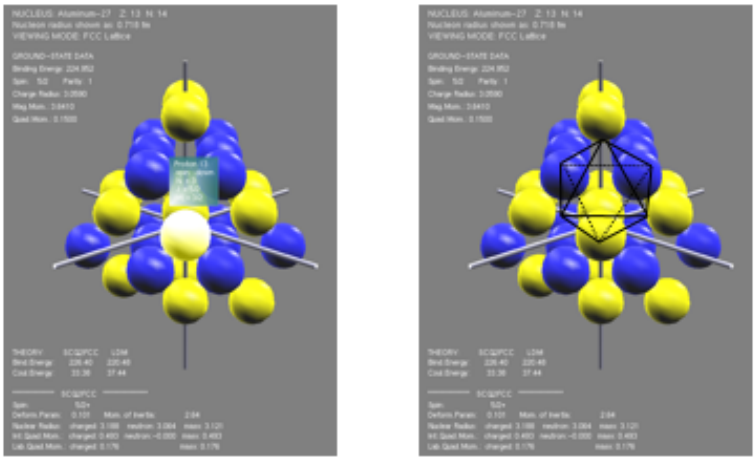

Figure 15: Left: The nucleus of ^{27}Al containing the proton with spin $5/2^+$ on d-shell (white colored). Right: This proton forms the virtual $\alpha-$cluster with the proton of s-shell and two neutrons of d-shell.

So far we have considered only even-even nuclei. However, the concept of virtual clusters is applicable to all nuclei: bound, excited, proton or neutron rich, high spin isomers etc. All even-even nuclei and most odd-even/even-odd ones are formed by virtual alphas, several odd-even/even-odd and all halo (neutron excess) nuclei include triton-like clusters. In the odd-even nucleus ^{27}Al the proton of d-shell with spin $5/2^+$ forms with the proton of s-shell two additional virtual alphas ((Fig. 15). One with two neutrons of d-shell and the other with two neutrons of p-shell (not shown as octahedron) that gives a total of 22 virtual alphas.

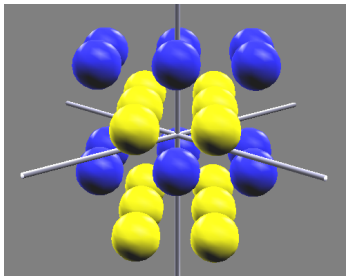

Figure 16: The ^{24}Mg nucleus consisting of two virtual ^{12}C clusters.

In some nuclei the virtual $\alpha-$clusters form more complex aggregations. For example, the most probable configuration of the ^{24}Mg nucleus can be represented as consisting of two ^{12}C nuclei, joined to each other by the virtual $\alpha-$clusters, even though they are both formed from the virtual alphas (Fig. 16). As we know from nuclear reaction experiments, heavy nuclei can release carbon nuclei as fragments during decay. In addition to (virtual) alpha clusters, some nuclei also contain three-nucleon virtual clusters. This applies mainly to some odd-odd nuclei and halo nuclei, i.e. proton- and neutron-rich nuclei. The light neutron-rich nuclei contain ^{3}H-like virtual clusters and proton-rich nuclei – ^{3}He-like ones. An example of such nuclei are helium isotopes ^{6}He and ^{8}He (Fig. 17) which are so-called borromean nuclei. A pair

of neutrons form the quark loop with the proton of the ^{4}He core producing virtual ^{3}H-like cluster. Coupling of neutrons to the ^{4}He core is similar to the borromean rings shown in the Figure. Breaking of any linkage in the loop leads to decay of the halo nucleus to its three parts.

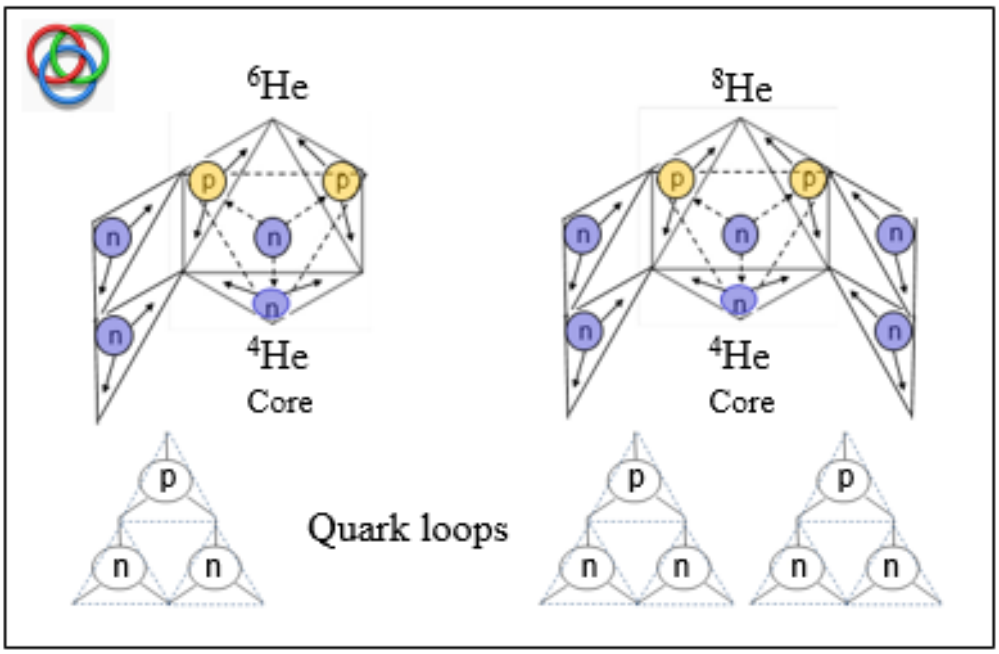

Figure 17: Halo isotops of helium, ^{6}He and ^{8}He which are the borromean nuclei. The bottom row shows quark loops appearing in the structure of triton (Fig. 2).

Thus, we have constructed the quark model of the nuclear structure based on quark loops that connect the free ends of colored quarks and allow us to describe nuclei with the closed shells as nested octahedral configurations. Further, it turned out that nucleons in such a scheme occupy the nodes of the FCC lattice. Considering nuclei with an unclosed shell, we found that quark loops lead to the formation of virtual three-nucleon (^{3}H- and ^{3}He-like) and four-nucleon (alpha-like) clusters. As a result, we can reformulate the model (SCQM), moving from quark considerations to the nucleon language, or more precisely, virtual clusters. Knowing the spin and parity of the nucleus, we can construct the nuclei of the periodic table of elements, gradually moving from light, to medium and then heavy and superheavy nuclei. All that is required of us is to track the formation of virtual ^{3}H-, ^{3}He-like and alpha-like clusters in the nuclear structure. All nuclei (except for odd-odd nuclei) and, in some cases excited ones, represent the structure formed due to virtual alpha clusters. To demonstrate this, we let's take the lead nucleus. It is an even-even, doubly magic, and last stable nucleus whose properties are well understood. That is why we will take it as an example to test the applicability of our model to reproduce the structure of nuclei and their properties. Comparison of the properties of ^{208}Pb obtained by the model to the experimental values is shown in Table 3: binding energy, B; spin; charged radius, R_{ch}; deformation parameter, β; electric quadrupole moment. We calculate the binding energy empirically using information about three closed-shell nuclei, ^{4}He, ^{16}O and ^{40}Ca: the binding energies, and the number of effective bonds per each nucleon. In ^{4}He the binding energy per nucleon is 7.07 MeV, and each

nucleon has 3 bonds which we count as effective. Then we calculate the number of effective bonds per each nucleon which can range from 2 (in deuteron) to 12 in ^{40}Ca and derive the bounding energy per nucleon with 3, 4, 5, 6, ..., 12 bonds. The number of 12 is specified by the maximum number of virtual alpha clusters surrounding one exchangeable nucleon. This number achieved for each $s-$shell nucleon in ^{40}Ca is 4. And since, the number of bonds in alpha-particle is 3, so the total number of effective bonds is 12. Thus, knowing the number of nucleons, number of effective bonds per each nucleon and binding energies per nucleons with 2, 3, 4, ... bonds we can estimate the binding energy of any nucleus. R_{ch} is calculated by the positions of protons plus the size of proton ($\sim$ 0.7 fm); the deformation parameter is defined as for a rigid body. Since the electric quadrupole moment of ^{208}Pb is zero, we give

Table 3: The properties of ^{208}Pb: binding energy, B; spin; charged radius, R_{ch}; deformation parameter, β; electric quadrupole moment, Q_{ch} (*in parenthesis - its intrinsic value Q_0).

	B, MeV	spin	R_{ch}, fm	β	Q_{ch}, barn
Exp.	1636.5	0^+	5.5		0
Model	1655	0^+	5.4	0.03	0 (-0.167)*

the value of the intrinsic quadrupole moment of the proton distribution Q_0, which is defined by the coordinates of protons

$$Q_0 = \sum \langle 2z_k^2 - x_k^2 - y_k^2 \rangle, \qquad k = 1, 2, ..., Z. \tag{14}$$

Using Q_0 we can calculate the measurable electric quadrupole moment Q_{ch} for nuclei with a spin J:

$$Q_{ch} = \frac{J(2J-1)}{(J+1)(2J+3)} Q_0. \tag{15}$$

In Figure 18 (a, b, c, d) we demonstrate the form of the ground state of the ^{208}Pb nucleus constructed according to the "virtual clusters" concept. As can be seen from the Figure, the shape of the nucleus significantly differs from spherical, although the value of the intrinsic quadrupole moment given by the model is quite close to zero. This is drastically different from the conclusion of the shell model about the sphericity of the doubly magic nucleus. Moreover, as can be seen from the Figure, neither the proton nor the neutron outer shells and subshells are filled. This is due, firstly, to the excess of neutrons over protons, and secondly, to the strong correlation of protons and neutrons, binding into virtual alpha clusters which form a configuration that corresponds to the maximum binding energy. Additional confirmation of the adequacy of the model in describing nuclear systems are panels **e** and **f** in the Figure demonstrating the transition of a neutron with spin $3/2^-$ from the shell with $n = 5$ to the shell with $n = 6$ in state $9/2^+$. As a result, ^{208}Pb transits from the ground state to the excited state with spin 3^-. This transition is described in textbooks in nuclear physics as an example of the transition of a nucleon from the lower shell to the upper one when the parity of a nucleus changes.

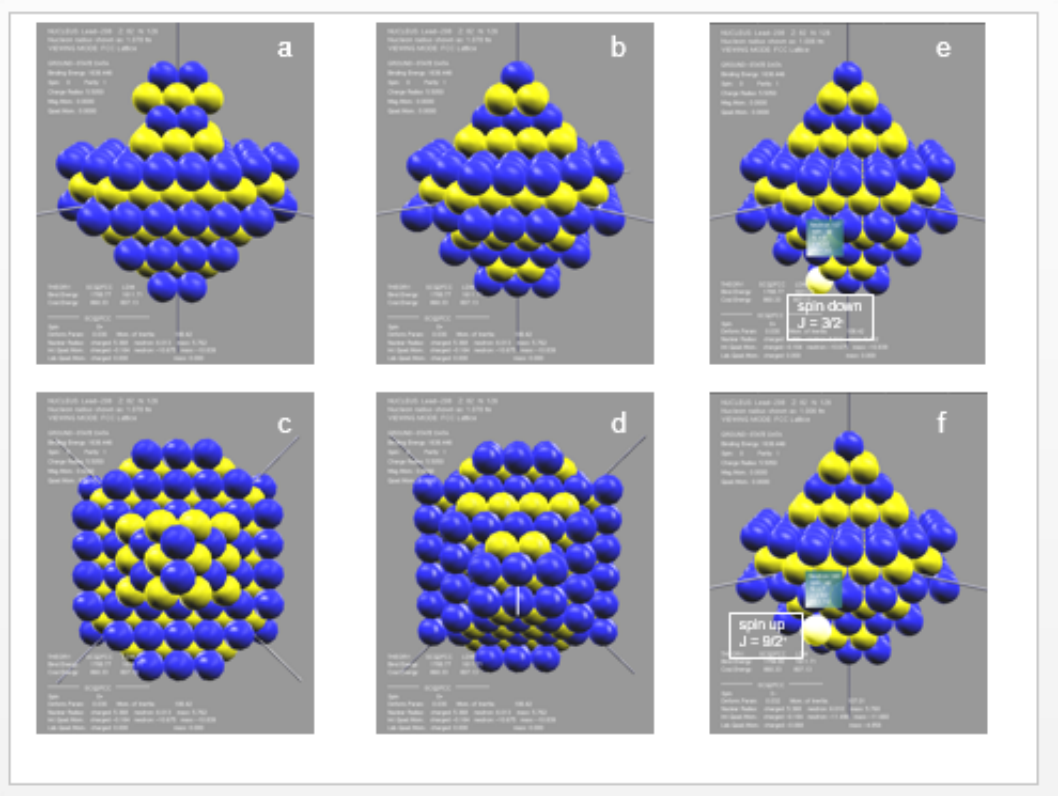

Figure 18: The nucleus of ^{208}Pb: panels **a**, **b**, **c**, **d** – different views of its ground state; **a**, **b** – two sides view, **c**, **d** – top and bottom view. Panels **e** and **f** show its transition from the ground state 0^+ (**e**), to the excited state 3^- (**f**).

6 Conclusion

The goal of our work was to answer the question of whether the quarks manifest themselves in the structure of the atomic nucleus. To address this problem, we formulated in Part I ([1]) the model of strongly correlated quarks, SCQM, based on SU(3) color symmetry, which we applied to construct the structure of nuclei. While doing so, we discovered that the binding between nucleons in the nucleus emerges through the formation of quark loops, which link the free ends of the colored quarks together. According to the model, nucleons are non-spherical, triangular shaped, three-colored objects, which is what creates these loops. The strongest binding between nucleons occurs when all the free ends of colored quarks are linked in loops, which is realized in the ^{4}He nucleus consisting of four nucleons bound by four loops. In analogy with the nucleus ^{4}He, in which four nucleons occupy in $s-$ shell, we build next two nuclei with shell closure, ^{16}O and ^{40}Ca. It turned out that nucleons take up positions on the sites of the face-centered-cubic lattice. Using a technique that relates lattice coordinates to shell model quantum numbers elaborated in [15], we can determine the spins and parities of all nucleons in our model. We then reformulated the model, moving from the quark language to the concept of virtual clusters, since quark loops lead to the formation of three- and four-nucleon virtual clusters in nuclei, which are ^{3}H-, ^{3}He- and ^{4}He-like clusters. The binding energy of an arbitrary nucleus is calculated empirically and determined by the number and strength of quark bonds and Coulomb repulsion. To estimate the strength of quark bonds, three nuclei with closed shells (He, O, Ca) were used as reference nuclei. This makes it

possible to estimate the binding energy of nuclei with an accuracy of 5-10%. To get a self-consistent theoretical description of the binding energy of nuclei, it is necessary to be able to calculate the depth of the potential well in the overlap region of the color quark fields of neighboring nucleons (Fig. 1), which also depends on the number of quark loops. Since color fields lead to the formation of quark-gluon condensate (see Part I), the problem of calculating the potential relates to describing the density of the condensate distribution around the valence quark. This requires knowledge of non-perturbative fluctuations in a physical vacuum. Such a description is not yet available and, possibly, can be estimated in the models of instanton vacuum [19, 20].

While choosing a particular configuration of nucleons in the nucleus, it is necessary to consider factors that influence the binding energy of the nucleus: the shape of the nucleus, type of deformation, moment of inertia, forces, etc. Further development of the model involves taking into account all factors affecting the binding energy of the nucleus. Currently we can construct the most probable configuration of any nucleus, including heavy and superheavy nuclei, halo nuclei, neutron/proton-rich nuclei, high spin isomers and so on. In the subsequent papers these nuclei and their properties will be analyzed in the framework of the model. Although at the moment the model is more qualitative, nevertheless it allows to make quantitative estimates. For example, the calculated nuclear sizes and their electrical quadrupole moments are consistent with experimental values within 5%. To summarize, we argue that the combined SCQM–FCC Lattice model can serve a reliable tool for studying the nuclear structure. The upcoming article will be devoted to the description of super-heavy nulcei.

References

[1] G. Musulmanbekov, Adv. Nucl. Sci. Appl. **1**, 105 (2025).

[2] G. Gamow, Proceedings of the Royal Society A **126** (803) 632–644 (1930).

[3] C.F. von Wiezsacker, Zeit. fur Phys. **96** 431 (1935).

[4] M.G. Mayer and J.H.D. Jensen, Elementary Theory on Nuclear Shell Structure (Wiley, New York, 1955).

[5] K. Ikeda, N. Tagikawa and H. Horiuchi, Prog. Theor. Phys., **464** (Suppl.) 464–475 (1968).

[6] A. Tohsaki, H. Horiuchi, P. Schuck, and G. Röpke, Phys. Rev. Lett. **87**, 192501 (2001).

[7] W. V. Von Oertzen, M. Freer, and Y. Kanada-En'yo, Phys. Rep. **432**, 43–113 (2006).

[8] V. Matveev and P. Sorba, IL Nuovo Cim. **45**, 257 (1978).

[9] J.S. McCarthy, I. Sick, R.R. Whitney, Phys. Rev. C **15**, 1396 (1977).

[10] E. Wigner, Phys. Rev. **51**, 106 (1937).

[11] N.D. Cook and V. Dallacasa, Phys. Rev. C **36**, 1883 (1987).

[12] K.J. Lezuo, Atomkernenergie **23**, 285 (1974).

[13] V. Dallacasa, Atomkernenergie **31**, 143 (1981).

[14] N.D. Cook and T. Hayashi, J. Phys. G: Nucl. Part. Phys. **23**, 1109 (1997).

[15] N.D. Cook and V. Dallacasa, Models of the Atomic Nucleus (2nd ed., Springer, Berlin, 2010).

[16] M. Gillard et al., Nucl. Phys. B **895**, 272 (2015).

[17] M. Gillard et al., Nucl. Phys. B **917**, 286 (2017).

[18] K.S. Krane, Introductory Nuclear Physics (Wiley, New York, 1988).

[19] R. Rajaraman, Phys. Rep. **21C**, 229 (1975).

[20] A.I. Vainshtein, V.I. Zakharov, V.A. Novikov and M.A. Shifman, Sov. Phys. Usp. **25**, 195 (1982).